

Unusually Small Electrical Resistance of Three-Dimensional Nanoporous Gold in External Magnetic Fields

T. Fujita,¹ H. Okada,^{2,3} K. Koyama,² K. Watanabe,² S. Maekawa,² and M. W. Chen^{1,2,*}

¹WPI Advanced Institute for Materials Research, Tohoku University, Sendai 980-8577, Japan

²Institute for Materials Research, Tohoku University, Sendai 980-8577, Japan

³Department of Physics, College of Humanities and Sciences, Nihon University, Tokyo 156-8550, Japan

(Received 3 July 2007; revised manuscript received 27 June 2008; published 16 October 2008)

We report the electric conductivity of three-dimensional (3D) nanoporous gold at low temperatures and in strong magnetic fields. It was found that topologically disordered 3D nanoporosity leads to extremely low magnetoresistance and anomalous temperature dependence as the characteristic length of nanoporous gold is tuned to be ~ 14 nm. This study underscores the importance of 3D topology of a nanostructure on electronic transport properties and has implications in manipulating electron transport by tailoring 3D nanostructures.

DOI: [10.1103/PhysRevLett.101.166601](https://doi.org/10.1103/PhysRevLett.101.166601)

PACS numbers: 72.15.-v, 72.80.Ng, 73.43.Qt, 75.47.-m

Electronic transport properties of nanostructured metals have been intensely studied in past 30 years, and various novel physical phenomena have been discovered, arising from finite size quantization effects and/or a large fraction of atoms in surface regions [1–5]. The transport properties of nanostructured metals generally show an unusual temperature dependence and an increase in residual resistivity with the decrease of characteristic lengths, such as nanograin size and film thickness, which has been interpreted in terms of an enhanced electron-electron interaction and electron scattering from interfaces and surfaces [6–8]. Among various nanostructured materials, nanoporous metals synthesized by chemical dealloying possess unique structure features that can be rationally described as a quasiperiodic network comprised of randomly oriented metallic nanowires and hollow nanochannels in 3D [9,10]. Although the transport properties of nanomaterials have been extensively investigated, the effect of 3D topology of nanostructures on electron transport remains fundamentally unknown. In this Letter, we report the electric conductivity of nanoporous gold (NPG) in strong magnetic fields at low temperatures. It was found that the resistivity of the complex 3D nanostructure follows Landau Fermi liquid theory, whereas the cyclotron motion of conduction electrons can be effectively suppressed by topologically disordered nanoporosity, resulting in extremely low magnetoresistance and anomalous temperature dependence.

The NPG films used in this study were prepared by chemically dealloying 100 nm thick $\text{Au}_{35}\text{Ag}_{65}$ (in at. %) gold leaf in 70 vol % HNO_3 for 5 min, 30 min, and 6 h at $\sim 25^\circ\text{C}$. The selective dissolution of silver results in the formation of NPG [11], and various dealloying times lead to the controllable nanopore sizes [12]. The resistivity measurements of NPG were performed using the standard four-probe technique from 0.5 to 300 K in magnetic fields (B) up to 18 T. The applied magnetic fields were either parallel or perpendicular to the current direction in order to evaluate the longitudinal and transverse magnetoresis-

tance. To retrieve the resistivity (ρ) from raw data, we quantitatively measured the volume fraction of gold ligaments in the three nanoporous samples using electron tomography [10]. The gold ligaments and nanopore channels are identical in both size and morphology (Fig. 1), and the fraction of gold ligaments in the nanoporous structure is ~ 50 vol %.

Figure 1 shows the micrographs of the three NPG specimens. An obvious size difference in nanopores and gold ligaments of the three specimens is readily identified. The average nanopore sizes of the three samples were precisely measured to be 14 ± 1 , 35 ± 3 , and 47 ± 3 nm,

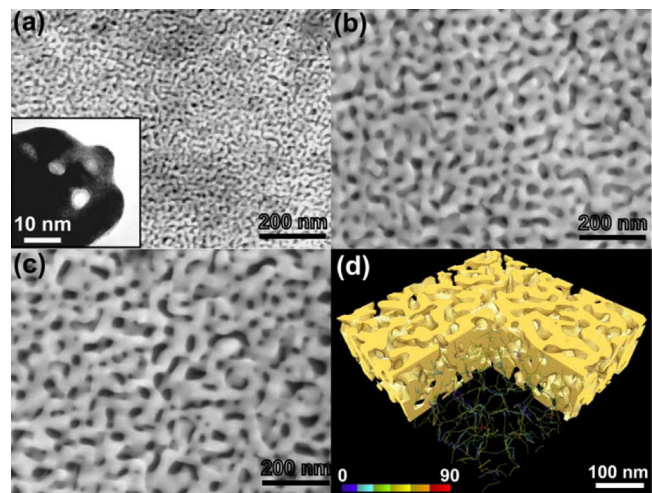


FIG. 1 (color online). Scanning electron microscope images of NPG with average pore sizes of (a) 14, (b) 35, and (c) 47 nm. The inset in Fig. 1(a) shows a TEM micrograph of the nanoporous sample. (d) 3D structure of the 14 nm sample imaged by electron tomography. A part of the 3D image is shown as the skeletal network of gold ligaments. The various colors of the skeletonized ligaments represent the deviation angles of the skeletonized ligaments from the z axis as indicated by the color bar from 0° (blue) to 90° (red).

respectively, using a rotational fast Fourier transform method [13]. Figure 1(d) shows an example of the 3D structure of NPG, revealed by electron tomography. The conduction channels, i.e., gold ligaments, are connected across the entire sample, but the directions of the ligaments are random, which results in a topological disorder [Fig. 1(d)].

Figure 2 shows the temperature dependence of the electric resistivity ρ of NPG with different nanopore sizes in zero magnetic fields. The electrical resistivity exhibits a simple metallic behavior down to 0.5 K, and the anomalous resistivity increase caused by electron localization due to the quantum size effect [14,15] has not been seen in the 3D nanostructure. The sample inhomogeneity is also not significant since the gold ligaments are fully connected across the samples for electron transportation [Fig. 1(d)]. The residual resistivities ρ_0 of the 14, 35, and 47 nm samples were measured to be 87.1, 35.7, and 28.8 n Ω m, respectively, and these absolute values of ρ_0 are about 2 orders of magnitude higher than that of bulk gold (0.22 n Ω m) [16]. Surprisingly, the resistivity of the complex 3D nanostructure can be well described by the Landau Fermi liquid theory [17]: $\rho = \frac{m^* v_F}{ne^2 l}$, where l is the mean free path, m^* is the effective carrier mass, v_F is the Fermi velocity, n is the carrier concentration, and e is the elementary charge. The mean free path l in the equation is associated with various scattering mechanisms. According to Matthiessen's rule, impurity scattering, phonon scattering, and interface scattering between gold ligaments and nanopore channels, all could be the possible scattering origins in NPG. To determine the mean free paths of the NPG samples, the product ρl of bulk pure gold equal to 0.96 f Ω m² [18] was used as the reference. Based on the measured ρ_0 , the calculated l of the nanoporous samples were estimated to be \sim 11, 27, and 33 nm, respectively, which are fairly close to the average nanopore sizes of 14, 35, and 47 nm (Fig. 1). Therefore, the electrical resistivity of NPG in the zero magnetic fields is dominated by the scattering from the interfaces between gold ligaments and nanopore channels [19–21]. Because the nanoporous structure is produced by selectively etching Ag from the Au₃₅Ag₆₅ alloy, more or less residual Ag is left in NPG. Careful chemical analysis demonstrates that the residual silver concentrations are \sim 8.6, 6.7, and 5.2 at. % in the 14, 35, and 47 nm samples, respectively. However, the impurity scattering effect arising from the residual Ag can be negligible because the measured mean free paths of NPG are much larger than that of the impurity scattering from the alien Ag atoms. Moreover, the resistivity vs temperature curves of NPG are approximately parallel to that of bulk pure gold (Fig. 2), indicating that the phonon scattering in NPG is the same as that in bulk gold. Thus, the increased resistivity with the decrease of nanopore size is mainly from the strong interfacial scattering of the 3D nanoporous structure.

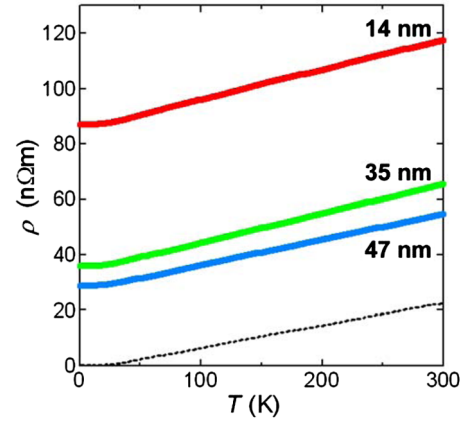


FIG. 2 (color online). Temperature dependence of the zero-field electrical resistivity of NPG with various nanopore sizes. Three respective profiles represent the results measured from the samples with the average nanopore (or gold ligament) sizes of 14, 35, and 47 nm, respectively. The dotted line represents the data of bulk gold [16].

Figure 3(a) illustrates the transverse and longitudinal magnetoresistance of the NPG samples with the pore sizes of 14 and 47 nm in the applied magnetic fields from 0 T up to 18 T at 4.2 K. The magnetoresistance is determined by the equation $\Delta\rho/\rho = [\rho(B) - \rho(0 \text{ T})]/\rho(0 \text{ T})$. Interestingly, the magnetoresistance of NPG is 1–2 orders of magnitude smaller than the known values of gold in the forms of bulk, nanowires, and thin films [5,22–26]. For an example, the magnetoresistance of 14 nm NPG is only \sim 0.1% in 18 T at 0.5 K, which is about 60 times smaller than that (\sim 6%) of gold thin films with a thickness of 93 nm in 9 T fields [26]. Moreover, in comparison with bulk gold, gold nanowires, and thin films, the diversity between transverse and longitudinal magnetoresistance of NPG is also very small and gradually reduces with nanopore sizes. As the nanopore size is down to 14 nm, a visible difference between the transverse and the longitudinal magnetoresistance cannot be seen (Fig. 3).

The magnetoresistance of NPG follows a linear function against B^2 as shown in Fig. 3(b), proving that the additional resistance to the flow of electrical currents in magnetic fields originates from the cyclotron motion of conduction electrons [27]. The important quantity of an electron cyclotron is the turn angle of the cyclotron motion in radians within a scattering lifetime, i.e., $\omega_c \tau$, where $\omega_c = eB/m^*$ is the cyclotron frequency and τ is the scattering lifetime of the conduction electrons. τ can be determined by the carrier mean free path $l = v_F \tau$. For gold, v_F is equal to 1.39×10^6 m/s [28]. Thus, $\omega_c \tau$ is estimated to be 2.2×10^{-2} , 5.3×10^{-2} , and 6.6×10^{-2} in 18 T for the 14, 35, and 47 nm NPG samples, respectively. It is known that the minimum requirement to observe a substantial magnetoresistance caused by the electron cyclotron motion is $\omega_c \tau \approx 1$. Apparently, the much smaller turn angles are responsible for the extremely low magnetoresistance of NPG. In other

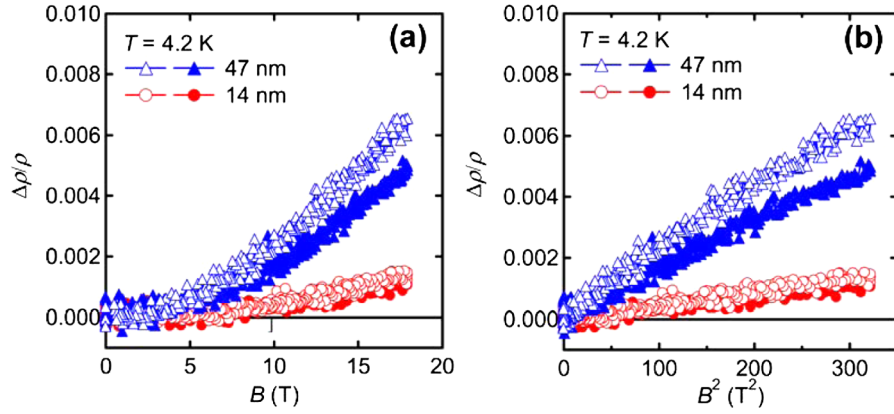


FIG. 3 (color online). Magnetoresistance of NPG. (a) Magnetoresistance effects of 14 and 47 nm NPG at 4.2 K. (b) B^2 dependence of magnetoresistance ($\Delta\rho/\rho$) at 4.2 K. The open and solid symbols show the transverse and longitudinal magnetoresistance, respectively.

words, the gold ligaments are much smaller than the cyclotron radius in bulk gold [for example, at 18 T $r_L = v_F/(eB/m^*) = v_F/\omega_c \approx 500$ nm]. Consequently, the nanoporous structure can effectively restrict the cyclotron motion of conduction electrons in the strong magnetic fields by the ligament-nanopore interface scattering and the disordered topology of gold ligaments. Although the residual Ag may affect the magnetoresistance of NPG, with the fact that the Hall effect constants of pure gold and Au-10 at. % Ag alloy are almost the same [29], the influence of the impurity Ag in the magnetoresistance of NPG can be negligible.

Figure 4(a) shows Kohler plots of the 47 nm nanoporous sample at various temperatures, i.e., $\Delta\rho/\rho$ plotted as a function of $B/\rho(0\text{ T})$ [27]. The nearly overlapping curves indicate that the magnetoresistance of NPG follows Kohler's rule although it has a very intricate 3D nanostructure. Moreover, at a constant temperature, for an example of 4.2 K, the magnetoresistance of nonporous gold with various nanopore sizes can be well scaled by Kohler's rule as shown in Fig. 4(b). Thus, the carrier density of NPG does not change with gold ligament sizes,

and the scattering lifetime $\omega_c\tau$ is mainly controlled by the ligament-nanopore interface scattering. Therefore, the observed nanosize effects in both the zero-field resistivity and the magnetoresistance of NPG result from the changes in scattering lifetime. It is worth noting that Kohler's rule is a result of the Fermi liquid theory and frequently does not work in complex metals, such as the various oxide metals (for example, high temperature cuprate superconductors), f electron alloys [30], and disordered alloys [31,32]. In general, chemical and structural disorder in amorphous metals and alloys can also suppress the cyclotron orbits of conduction electrons by quantum localization [31,32]. However, the signature of electron localization in NPG has not been detected in both low and high magnetic fields. Thus, our finding is intrinsically different from the traditional atomic-scale disorder effect on magnetoresistance. The new type of disorder in the bottom-up type of nanoporous structure can hold a Fermi liquid picture but has an effect on cyclotron orbits.

Generally, ordinary magnetoresistance of metals is strongly dependent on measured temperatures and becomes more significant at lower temperatures due to the

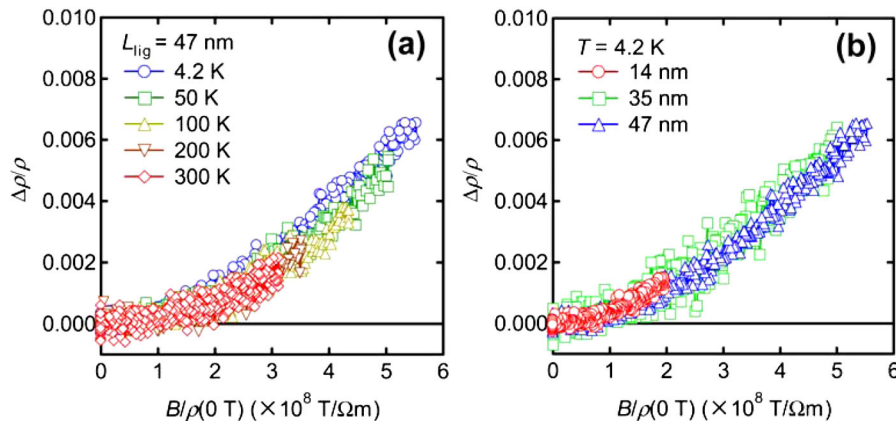


FIG. 4 (color online). Kohler plotting of NPG. (a) Kohler plottings of the 47 nm nanoporous sample at various temperatures. (b) Kohler plottings of 14, 35, and 47 nm nanoporous samples at 4.2 K.

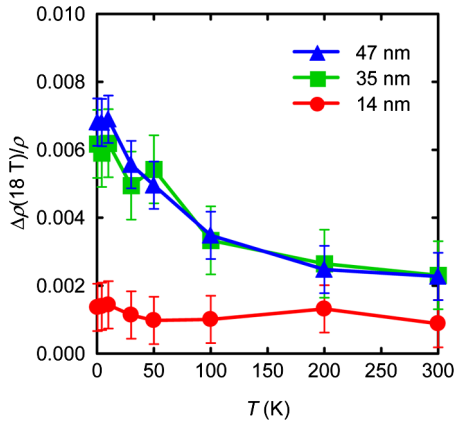


FIG. 5 (color online). Temperature dependence of magnetoresistance of NPG in 18 T magnetic fields. The 14 nm nanoporous sample exhibits anomalous temperature independence in magnetoresistance.

decrease of thermal phonon scattering. The nanoporous samples with pore sizes of 35 and 47 nm follow the same tendency as shown in Fig. 5. Nevertheless, the 14 nm nanoporous sample exhibits unusual behavior. The extremely low magnetoresistance, less than 0.2%, has a very weak temperature dependence and keeps approximately constant across the entire temperature range from 0.5 to 300 K (Fig. 5). This anomalous temperature dependence combining with the extremely low magnetoresistance suggests that the 14 nm nanopore size appears to approach a critical value at which the magnetoresistance caused by the cyclotron motion of conduction electrons can be completely suppressed by the strong interface scattering and by the topological disorder of the 3D nanoporosity. As shown in Fig. 2, the increment of $\rho(0\text{ T})$ from 0.5 to 300 K is $\sim 25\text{ n}\Omega\text{ m}$ for both NPG and bulk gold. However, the residual resistivities ρ_0 dramatically increase from 0.22 n $\Omega\text{ m}$ of bulk gold and 28.8 n $\Omega\text{ m}$ of 47 nm NPG to 87.1 n $\Omega\text{ m}$ of 14 nm NPG. Therefore, as the nanopore size is down to 14 nm, the additional dynamic disorder introduced by the presence of thermal phonons has relatively little influence on the resistivity, which is already high as a result of the scattering caused by the static interface scattering. Assuming the resistivity increment caused by magnetic fields is independent of temperature [Fig. 4(a)], as temperature decreases from 300 to 0.5 K, the magnetoresistances of bulk gold and 47 nm NPG increases ~ 100 and 2 times, respectively, whereas for 14 nm NPG the temperature-induced magnetoresistance increment is only $\sim 30\%$, and thus this sample shows very weak temperature dependence.

In summary, we found that the magnetoresistance of NPG is extremely low in strong magnetic fields at low temperatures, revealing that nanosized gold ligaments with disordered topology can effectively restrict the cyclotron motion of conduction electrons in strong magnetic fields.

Moreover, the electronic state of NPG with a complex 3D nanostructure can be well described by the Fermi liquid theory. Therefore, the 3D nanoporosity can hold a Fermi liquid picture but has an effect on cyclotron orbits, showing a new type of disorder effect in magnetoresistance.

*Corresponding author.

mwchen@imr.tohoku.ac.jp

- [1] M. N. Baibich *et al.*, Phys. Rev. Lett. **61**, 2472 (1988).
- [2] H. Hegger *et al.*, Phys. Rev. Lett. **77**, 3885 (1996).
- [3] Y. Guo *et al.*, Science **306**, 1915 (2004).
- [4] A. I. Yanson, I. K. Yanson, and J. M. van Ruitenbeek, Nature (London) **400**, 144 (1999).
- [5] E. Scheer *et al.*, Phys. Rev. Lett. **78**, 3362 (1997).
- [6] H. Gleiter, Prog. Mater. Sci. **33**, 223 (1989).
- [7] G. Fishman and D. Calecki, Phys. Rev. Lett. **62**, 1302 (1989).
- [8] G. Reiss, J. Vancea, and H. Hoffmann, Phys. Rev. Lett. **56**, 2100 (1986).
- [9] H. Roesner *et al.*, Adv. Eng. Mater. **9**, 535 (2007).
- [10] T. Fujita *et al.*, Appl. Phys. Lett. **92**, 251902 (2008).
- [11] A. J. Forty, Nature (London) **282**, 597 (1979).
- [12] L. H. Qian and M. W. Chen, Appl. Phys. Lett. **91**, 083105 (2007).
- [13] T. Fujita and M. W. Chen, Jpn. J. Appl. Phys. **47**, 1161 (2008).
- [14] P. Chaudhari, H.-U. Habermeier, and S. Maekawa, Phys. Rev. Lett. **55**, 430 (1985).
- [15] A. Palevski and G. Deutscher, Phys. Rev. B **34**, 431 (1986).
- [16] R. A. Matula, J. Phys. Chem. Ref. Data **8**, 1147 (1979).
- [17] A. A. Abrikosov, *Fundamentals of the Theory of Metals* (Elsevier, New York, 1988).
- [18] J. R. Sambles, K. C. Elsom, and D. J. Jarvis, Phil. Trans. R. Soc. A **304**, 365 (1982).
- [19] E. H. Sondheimer, Phys. Rev. **80**, 401 (1950).
- [20] R. C. Munoz *et al.*, Phys. Rev. Lett. **96**, 206803 (2006).
- [21] I. B. Bhattacharya and D. L. Bhattacharya, Int. J. Electron. **41**, 285 (1976).
- [22] J. E. Huffman, M. L. Snodgrass, and F. J. Blatt, Phys. Rev. B **23**, 483 (1981).
- [23] C. P. Umbach *et al.*, Phys. Rev. B **30**, 4048 (1984).
- [24] P. M. Echternach and H. M. Bozler, Phys. Rev. B **44**, 10905 (1991).
- [25] S. Friedrichowski and G. Dumpich, Phys. Rev. B **58**, 9689 (1998).
- [26] R. C. Munoz *et al.*, Phys. Rev. B **74**, 233402 (2006).
- [27] J. M. Ziman, *Electrons and Phonons* (Oxford University Press, London, 1963).
- [28] C. Kittel, *Introduction to Solid State Physics* (Wiley, New York, 2005), 8th ed., Chap. 6, p. 139.
- [29] N. V. Grum-Grzhimailo, Russ. J. Inorg. Chem. **9**, 2048 (1956).
- [30] P. W. Anderson, Phys. Rev. Lett. **67**, 2092 (1991).
- [31] E. Abraham *et al.*, Phys. Rev. Lett. **42**, 673 (1979).
- [32] M. A. Howson and B. L. Gallagher, Phys. Rep. **170**, 265 (1988).